

Article

Influence of Complex Service Factors on Ravelling Resistance Performance for Porous Asphalt Pavements

Zhihao Cheng^{1,2,3}, Shaopeng Zheng^{2,3,*}, Naixing Liang¹, Xiao Li^{2,3}  and Libin Li²¹ School of Civil Engineering, Chongqing Jiaotong University, Chongqing 400074, China² Broadvision Engineering Consultants, Kunming 650000, China³ Yunnan Key Laboratory of Digital Communications, Kunming 650000, China

* Correspondence: zsp060324@163.com

Abstract: The study aims to analyze the influence of complex service factors on ravelling resistance performance for large-void asphalt pavements by carrying out tests on environmental and vehicle factors, conducting ultraviolet aging, freeze–thaw cycles, as well as vehicle speed simulated tests with the Rotating Surface Abrasion Test, vehicle tests, and traffic volume tests, and by making a correlation analysis between the Cantabro Abrasion test and Rotating Surface Abrasion Test. The result shows that environmental factors significantly affect the ravelling resistance performance of drainage asphalt pavements. With the increase in the times of UV aging and freeze–thaw cycles, the ravelling loss rate of asphalt specimens shows a tendency to increase, and the combined test of UV aging and freeze–thaw cycles aggravated the ravelling damage of asphalt specimens. Meanwhile, vehicle factors have a significant attenuation effect on the ravelling resistance performance of drainage asphalt pavements. With the increase in the speed, pressure, and times of the Rotating Surface Abrasion, the ravelling loss rate of asphalt specimens shows a steady tendency to increase. Furthermore, there exists a good correlation between the Rotating Surface Abrasion speed, pressure, times, and the ravelling loss rate. Finally, the two test results of the Cantabro Abrasion test and Rotating Surface Abrasion test are consistent in their changes during single/composite factor analysis, confirming the feasibility of using the Rotating Surface Abrasion test index to characterize the change in the ravelling resistance performance of drainage asphalt pavements.



Citation: Cheng, Z.; Zheng, S.; Liang, N.; Li, X.; Li, L. Influence of Complex Service Factors on Ravelling Resistance Performance for Porous Asphalt Pavements. *Buildings* **2023**, *13*, 323. <https://doi.org/10.3390/buildings13020323>

Academic Editors: Huayang Yu and Tao Wang

Received: 9 December 2022

Revised: 10 January 2023

Accepted: 17 January 2023

Published: 21 January 2023



Copyright: © 2023 by the authors. Licensee MDPI, Basel, Switzerland. This article is an open access article distributed under the terms and conditions of the Creative Commons Attribution (CC BY) license (<https://creativecommons.org/licenses/by/4.0/>).

Keywords: drainage asphalt pavement; stripping performance; UV aging; freeze–thaw cycles; coupling analysis

1. Introduction

As cities expand, they are more vulnerable to flooding because impervious surfaces are completely unable to absorb rainfall. Therefore, both mild and catastrophic floods are becoming more and more likely to occur [1]. The flooding has affected people's lives, businesses, and whole societies, not to mention the cost of damage. In recent years, porous asphalt pavements (PA), as an effective sustainable drainage system, have been increasingly promoted to alleviate surface floods in the motorways and expressways [2]. The porosity of permeable pavements is as high as 15–20%, or even more than 20%, while that of the traditional asphalt pavement is only 3–6%. Because of its large gap, rainwater can penetrate into the pavement and drain from the connected pores in the pavement to the edge of the pavement [3,4]. However, the pore structure of porous asphalt pavements may be blocked by sediment particles, and its ability to discharge rainwater runoff may gradually decrease [5]. Early research on PA was mainly limited to the relationship between asphalt performance, mixture gradation, and drainage performance. The research shows that various properties of asphalt and aggregate have an impact on PA, and lays a foundation for the development and improvement of PA [6]. However, these studies often focus on the composition of the foundation. The types of asphalt and aggregate are limited and the important drainage function has not received much attention [7,8].

During the service life of asphalt pavements, due to asphalt aging, dynamic water erosion, and heavy load, some pavement damage may occur continuously, such as loose, brittle cracking, pitting, etc., thus, significantly reducing the service life of asphalt pavements [9,10]. Because porous asphalt layers have a large number of pores, under the influence of heavy traffic load and complex climate, some typical damage such as looseness, rutting, and cracking often occurs [11,12]. Xu's investigation on the application of OGFC in the United States shows that the most serious problem in the porous asphalt wearing course is looseness, which may significantly reduce the expected life of porous asphalt pavements [13]. Miradi reported the test results of the durability study of the porous asphalt wearing course. They found that the degree of looseness of porous asphalt mixtures will increase with the increase in pavement service time. Once loose damage occurs in a certain area of a porous asphalt mixture, the loosening of the surrounding aggregate will accelerate and eventually lead to serious pavement damage [14]. Compared with densely graded asphalt mixtures, porous asphalt mixtures have lower strength and rutting resistance. For the densely graded asphalt ultra-thin wearing course, it can prevent oxygen and moisture from entering the asphalt pavement, reduce asphalt aging, and effectively delay the appearance of pavement damage [15]. However, with the application of the porous asphalt ultra-thin wearing course, the influence of oxygen and moisture on it is more evident because its porosity is large and the paving thickness is thin, resulting in loose, brittle cracking, pitting, or a combination of the two. Compared with densely graded asphalt pavements with a service life of about 18 years, the average thickness of porous asphalt pavements has been limited to 10–12, or even shorter, for many years [1,16].

The porous asphalt pavement, characterized by its large voids and lower content of fine aggregates, is susceptible to natural aging. With vast areas of the pavement immersed in water for a long time (with water on vast areas of the pavement for a long time), the asphalt mixture is prone to more intense damage caused by water, so ravelling has become one of the main defects of porous asphalt pavements. The fast movement of vehicles on large-void asphalt pavements, coupled with environmental factors, is more likely to cause ravelling and stone loss of drainage asphalt pavements in a complex service environment [17].

The main influencing factors of the ravelling resistance performance of drainage asphalt pavements can be classified into two categories: environmental factors including heat, light, temperature, water, etc., and vehicle factors including vehicle operating speed, vehicle load, traffic volume, etc. [18]. The ravelling resistance performance of large-void asphalt pavements has been of immense interest to researchers. Mousavi et al. investigated the mechanism of aggregate spalling under the coupling effect of UV aging and freeze–thaw cycles for different mixtures [19,20]. Dan et al. studied the effect of high-temperature aging and freeze–thaw cycles on the ravelling resistance performance of drainage asphalt pavements [13,21]. Vallerga et al. argued that asphaltic materials were susceptible to weathering in the presence of ultraviolet radiation, making the ravelling resistance and other road performances of asphalt pavements deteriorate rapidly [22]. This view was confirmed by some researchers [23,24]. Kouko et al. concluded that binders had a significant effect on the ravelling characteristics of drainage asphalt pavements. Minegishi et al. related the ravelling characteristics of drainage asphalt pavements to traffic loads [25]. The research conducted by Lucinda et al. showed that the early deterioration of the ravelling resistance performance of asphalt pavements was mainly caused by cohesion and adhesion damage (cohesion failure and adhesion failure) [26,27].

The ravelling resistance performance of porous asphalt pavements is mainly affected by temperature, material aging, vehicle load, wheel speed, traffic volume, and other factors [28]. Therefore, the analysis of the influence of various complex factors on the ravelling resistance performance of drainage asphalt pavements helps build a good architectural model for improving and upgrading the ravelling resistance performance of drainage asphalt pavements, establishing a clear system for long-term performance prediction and evaluation, and providing the foundation for decision making in large-scale functional road maintenance [29]. The Cantabro test is the standard asphalt mixture stripping test specified

in China’s current “Highway Engineering Asphalt and Asphalt Mixture Test Procedure” (JTG E20-2011) [30]. However, there is no relevant data available to support the correlation between the independently developed Rotating Surface Abrasion test (a new test method for porous asphalt in general investigating mechanical stability) and the standard specification test. Therefore, it is of great significance to compare the Cantabro Abrasion test with the Rotating Surface Abrasion test to explore the correlation between the two, promote the application of the self-developed equipment, and to study the evolution of the ravelling resistance performance of drainage asphalt pavements under actual operating conditions.

Due to its larger void rate, drainage asphalt pavements are more susceptible to environmental impact than densely graded asphalt pavements, especially in highland mountainous areas with intense ultraviolet radiation. The reason is that in these areas the texture depth (MTD) of the pavement surface is greater, so the ultraviolet radiation will cause the surface of the asphalt mixture to age even more. With all the factors taken into consideration, it was found that the drainage asphalt pavement was not suitable for such places because this kind of pavement is very susceptible to temperature changes and rainwater damage. Furthermore, large-void porous asphalt pavements have the function of internal drainage (inner drainage). Hot weather and water erosion will, to a certain extent, accelerate the ravelling and aggregate loss of the pavement. Based on this, the research on the ravelling resistance performance of large-void asphalt pavements is carried out under complex factors by simulating natural aging effect and temperature–water damage through UV aging and freeze–thaw cycles, coupled with vehicle loading factors, to provide the experimental and theoretical basis for the long-term service performance of large-void asphalt pavements.

2. Materials and Methods

2.1. Raw Materials

The asphalt used in this study was SBS-modified asphalt made with aggregate crushed from basalt, limestone mineral powder, and the high viscosity modifier HVA-III. HVA-III is a composite asphalt modifier formed through the prilling process (prilling process) with epoxy-based viscosity-enhancing resin, thermoplastic elastomer, ravelling resistance agent, and antioxidant, whose performance has a direct bearing on the interface bonding performance of the aggregate gradation. Its main technical indicators are shown in Table 1.

Table 1. Technical index of high viscosity additive.

Appearance	Single Particle Mass/g	Density/g/cm ³	Melting Index/g/10 min
Even-grained, full-grained	≤0.03	0.90~1.00	≥20

The aggregate gradation of the PA-13 used in the test is shown in Table 2. The total amount of asphalt and high viscosity agent was 4.6%, the ratio of the two materials was 9:1, and the amount of asphalt and high viscosity agent was 4.14% and 0.46%, respectively. The mineral powder accounted for 3% of the total amount of the aggregate. The asphalt–aggregate ratio of the PA-13 asphalt mixture was 4.82, and the air void of asphalt Marshall specimens and trapezoidal rutting plate specimens were controlled within 20% ± 0.5%.

Table 2. Aggregate composite gradation.

Sieve Size/mm	13.2	9.5	4.75	2.36	1.18	0.6	0.3	0.15	0.075
Passing rate by mass/%	88.66	57.51	25.59	14.58	10.95	9.88	7.86	6.58	5.49

2.2. Test Methods

2.2.1. UV Aging Test

In order to carry out the UV aging test, test conditions of 8 h exposure (black plate temperature of 60 °C) plus 4 h condensation (black plate temperature of 50 °C) were

determined, and UVA340 lamp UV irradiance was set at $1 \text{ W/m}^2 \times \text{nm}$ with a control wavelength of 340 nm. Moreover, 8 h light + 4 h condensation for one cycle was determined in this UV aging test. The test equipment and method are shown in Figure 1.

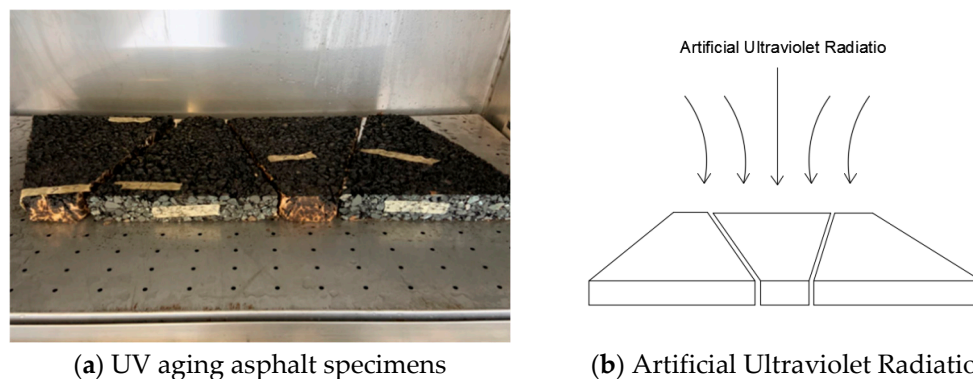


Figure 1. UV aging test.

2.2.2. The Freeze–Thaw Cycle Test

Concerning the relevant provisions of the “Test Procedure for Asphalt and Asphalt Mixture for Highway Engineering” (JTG E20-2011) in China, the immersion Marshall test (T0709) (Immersion Marshall test) and the freeze–thaw split test (T0729) (freeze–thaw splitting test) were employed to evaluate the effects of temperature–water factors on the ravelling resistance performance of drainage asphalt pavements. Since standard Marshall specimens and unconventional trapezoidal specimens were used in this test, the freeze–thaw cycle test was deliberately improved in this study. In the test, the specimen’s surface was ensured to undergo a complete freeze–thaw cycle process and experience different types of freeze–thaw cycles to conform to different test requirements. The specimens were immersed in water for 1 h at room temperature ($20 \text{ }^\circ\text{C} \pm 0.5 \text{ }^\circ\text{C}$), frozen at $-18 \text{ }^\circ\text{C}$ for 16 h, and then taken out to put into water at $60 \text{ }^\circ\text{C}$ for 24 h before immersing into water at $25 \text{ }^\circ\text{C}$ for another 2 h, which was defined as one complete freeze–thaw cycle process in this test. During the test, the UV aging cycle test was applied to the standard Marshall specimens, followed by the freeze–thaw cycle test, with 3, 6, and 9 cycles for the UV aging test, and 1, 2, and 3 cycles for the freeze–thaw cycle test, respectively, so as to analyze the dual damage of the two aging tests on the drainage asphalt pavement material. The test method is shown in Figure 2.

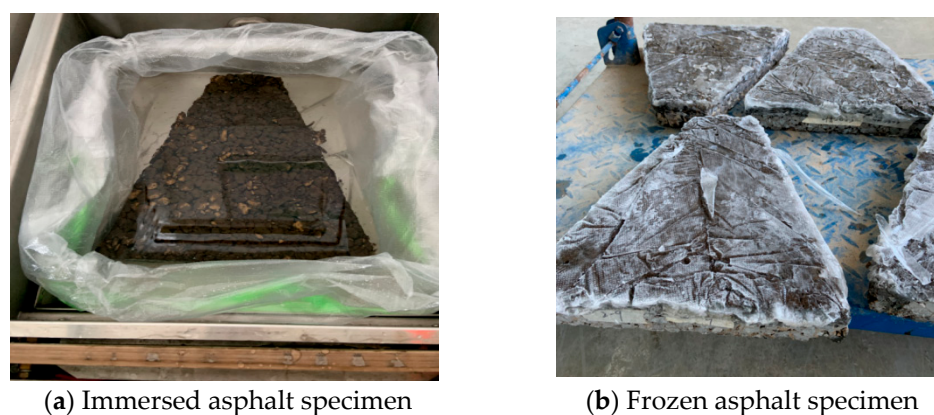


Figure 2. Specimens in the freeze–thaw cycle test.

2.2.3. The Cantabro Test

The Cantabro test (JTG E20-2011 T0733) was selected to evaluate the ravelling resistance performance of porous asphalt pavements in which the standard Marshall specimens evaluated by the Cantabro test. In this test study, the mass-loss rate of specimens (%) served

as the primary evaluative index, and the extent of surface damage of specimens as the auxiliary. The Cantabro test is the specified standard test performed in a cylinder with a length, width, and height of 1100 mm \times 780 mm \times 1000 mm, respectively, running at 30 r/min for 10 min, experiencing a total of 300 rolling rounds. In the test, radiation intensity was set to give UV irradiation and condensation treatment to standard asphalt mixture Marshall specimens, with the void rate of all specimens controlled within $20\% \pm 0.5\%$ to avoid the negative impact of the void rate on the test results. After the specified times of the UV aging tests, the asphalt Marshall specimens were broken down at an accelerated speed by using the Cantabro Abrasion test method. The Cantabro test method is shown in Figure 3.

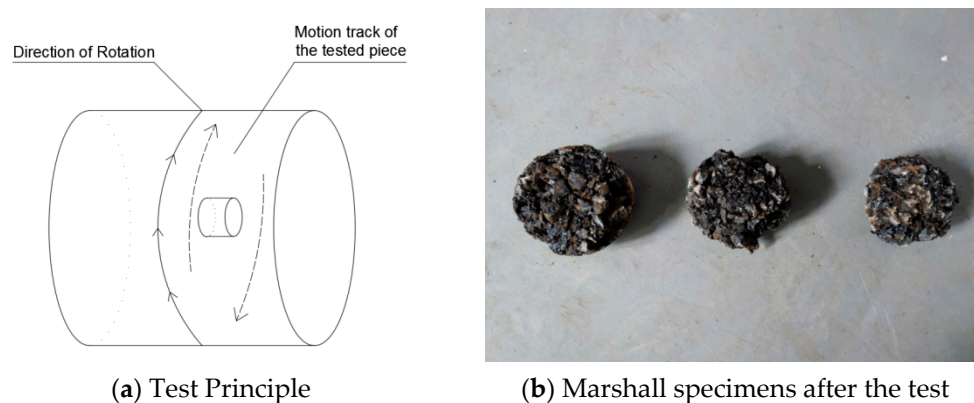


Figure 3. Cantabro test.

2.2.4. Rotating Surface Abrasion Test

The RSAT (self-developed) was selected to evaluate the ravelling resistance performance of porous asphalt pavements, and asymmetric trapezoidal plate specimens were also evaluated by the RSAT. In this test study, the mass-loss rate of specimens (%) served as the primary evaluative index, and the extent of the surface damage of specimens as the auxiliary. The self-developed RSAT equipment mainly contains a wheel control system, power control system, and ambient temperature control system, which can simulate the vehicle running speed, vehicle load, and traffic volume by adjusting the wheel running speed, exerting pressure, and adding running times to do the test study on the influence of vehicle factors on the ravelling resistance performance of drainage asphalt pavements. Three groups of parallel specimens were selected to collect data during the study, and the average values of the three groups of parallel tests were used as the basis for analysis. The Rotating Surface Abrasion test was conducted by using trapezoidal plates with their top and bottom measured at 80 mm and 300 mm, respectively, and their height and thickness of 300 mm and 50 mm, respectively. The air void of the asphalt mixture's trapezoidal plates was kept consistent with that of standard Marshall specimens, which was controlled within $20\% \pm 0.5\%$ to ensure the consistency of the test conditions. In this test, the differentiated effect of vehicle factors on the ravelling resistance performance of drainage asphalt pavements was investigated by varying the rotating speed of the Rotating Surface Abrasion equipment to simulate the vehicle speed test, adjusting the pressure applied to the equipment to simulate the vehicle load test, and simulating the traffic volume test with different Rotating Surface Abrasion times.

Before the Rotating Surface Abrasion test, the trapezoidal plate specimen was subjected to the UV aging test 9 times and the freeze–thaw cycle test 3 times. In the Rotating Surface Abrasion test, the pressure of the Rotating Surface Abrasion equipment was fixed at 160 kg, the Rotating Surface Abrasion rotation times were set at 30,000, and the rotating speed of the equipment was adjusted to 40 r/min, 60 r/min, 80 r/min, and 100 r/min, respectively, to simulate different vehicle driving speeds.

In the simulated vehicle load test, the trapezoidal plate was subjected to the UV aging test 9 times and the freeze–thaw cycle test 3 times as well. After that, the Rotating Surface

Abrasion speed was fixed at 100 r/min, the number of rotations was set at 30,000 times, and the Rotating Surface Abrasion loading force was set at 40 kg, 80 kg, 120 kg, and 160 kg, respectively, for simulating different vehicle tests.

In the simulated traffic volume test, the UV aging test was applied 9 times and the freeze–thaw cycle test 3 times to the trapezoidal specimens as well. After that, the Rotating Surface Abrasion test pressure was fixed at 160 kg and the Rotating Surface Abrasion speed was set at 100 r/min. The traffic volume test was simulated by adjusting different rotating times, with the rotating times set at 5000, 10,000, 20,000, and 30,000, respectively.

The Rotating Surface Abrasion Test method is shown in Figure 4.

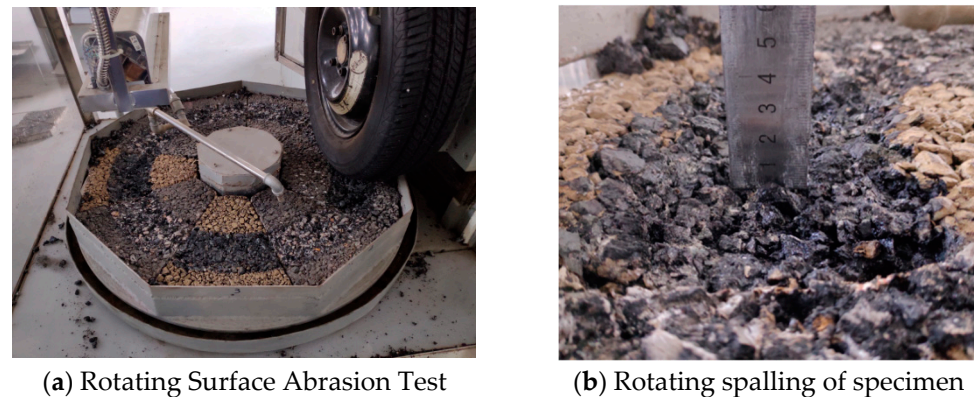


Figure 4. Rotating Surface Abrasion Test.

3. Results and Analysis

3.1. The Impact of Environmental Factors on the Ravelling Resistance Performance of Drainage Asphalt Pavements

3.1.1. UV Aging Cycle Test

The mass-loss rate of the specimens was recorded after ravelling was used as the evaluative index, and the test results are shown in Figure 5.

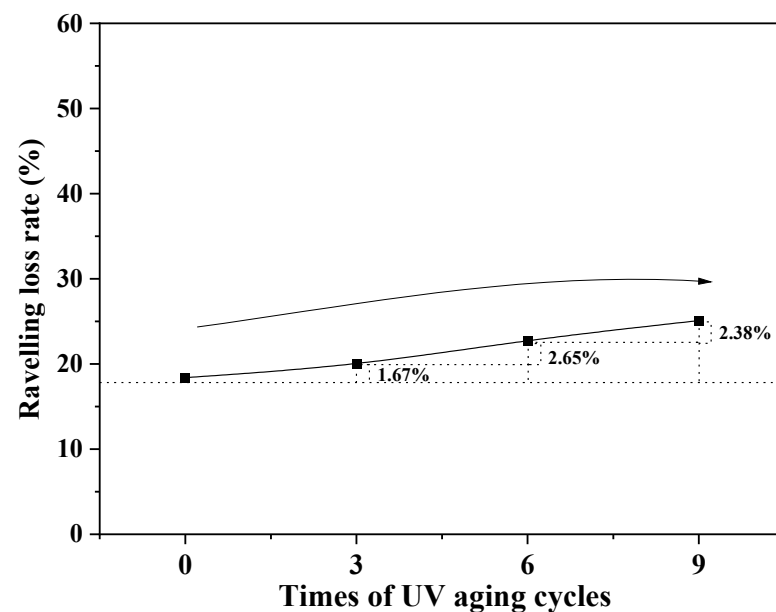


Figure 5. Effect of the UV aging cycle test on the ravelling resistance performance of asphalt mixtures.

The test results show that with UV aging cycles increasing steadily the mass ravelling loss rate of Marshall specimens is on the rise. In the study, the UV aging cycle was designed three, six, and nine times. The analysis in Figure 5 shows that after three and zero UV aging

cycles the difference between the specimen ravelling loss rate in these two tests was 1.67%, the specimen ravelling loss rate after six and three UV aging cycles was 2.65%, and the specimen ravelling loss rate after nine and six UV aging cycles was 2.38%, which reveals that the influence of the times of UV aging on the loss rate of specimens tends to decrease after increasing for some time. This result shows that the specimen ravelling loss rate is affected, to a certain extent, by the times of UV aging cycles, which increases first and then decreases.

Based on the analysis, the materials of the Marshall specimens were spalled and damaged in the UV aging cycle test, mainly because the UV aging could destroy the interfacial adhesion between the asphalt binder and the aggregate, causing the mass loss of the aggregate in the ravelling test as it was knocked to spall easily. At the same time, due to the complex structure of the asphalt mixture, the aggregate and the UV-aged asphalt binder would, to a certain extent, delay or prevent the further aging inwards, which could explain the reason for the decrease in the impact of specimen ravelling loss rate as the times of UV aging increased [31]. A lot of test data and specimen damage morphologies also prove this point. It is generally believed that UV aging has the greatest impact on about one centimeter from the surface of the asphalt mixture. (Figure 4b shows the results of the test data).

3.1.2. Freeze–Thaw Cycle Test

Large-void asphalt pavements are used in warm and humid areas with abundant rainfall. However, heavy rain lasting for a long time over a wide area, compounded by extremes of temperature, will accelerate the degree of attenuation in the ravelling resistance performance of drainage asphalt pavement materials, thus, affecting their service life. This study couples water immersion and freezing tests to impose aging damage behavior on specimens in an exploration of the changes of ravelling resistance performance of drainage asphalt pavement asphalt mixtures under freeze–thaw cycle tests.

The test results, as shown in Figure 6, indicate that with the increase in the times of freeze–thaw cycles the mass ravelling loss rate of specimens increases steadily. The data in the Figure shows that after three freeze–thaw cycles, compared with the specimens not treated, the ravelling loss rate increased by 24.31%, and every additional time of the freeze–thaw cycle would increase the specimen mass ravelling loss rate by about 8.10%. It can also be analyzed that after two freeze–thaw cycles every additional time of the freeze–thaw cycle would, on average, increase the ravelling loss rate by 7.55%, while the increase in specimen mass ravelling loss rate was 4.44% after only one freeze–thaw cycle test. It can be seen that with the increase in the times of freeze–thaw cycles the asphalt Marshall specimen internal damage will gradually increase, resulting in a corresponding increase in the mass-loss rate after the ravelling test.

The comparison between the results of the freeze–thaw cycle test (Figure 6) and UV aging cycle test (Figure 5) reveals that after three freeze–thaw cycles the Cantabro ravelling loss rate of asphalt Marshall specimens reaches 42.71%, while after nine UV aging cycles the Cantabro ravelling loss rate of specimens is only 25.10%, indicating a stronger damage effect of freeze–thaw cycle test on specimens than that of the UV aging test. In the freeze–thaw cycle test, the porous asphalt pavement was repeatedly immersed and frozen to produce a greater damage effect on the interfacial adhesion of the asphalt test specimen. Furthermore, a large frost heave stress could be observed in the interior of test specimens, which resulted in intensified damage to the specimen. However, the UV aging test had a greater impact on the surface of the specimen but a weaker influence on the interior of the specimen, leading to a bigger difference in the impact of the two tests on the asphalt specimen's ravelling resistance performance.

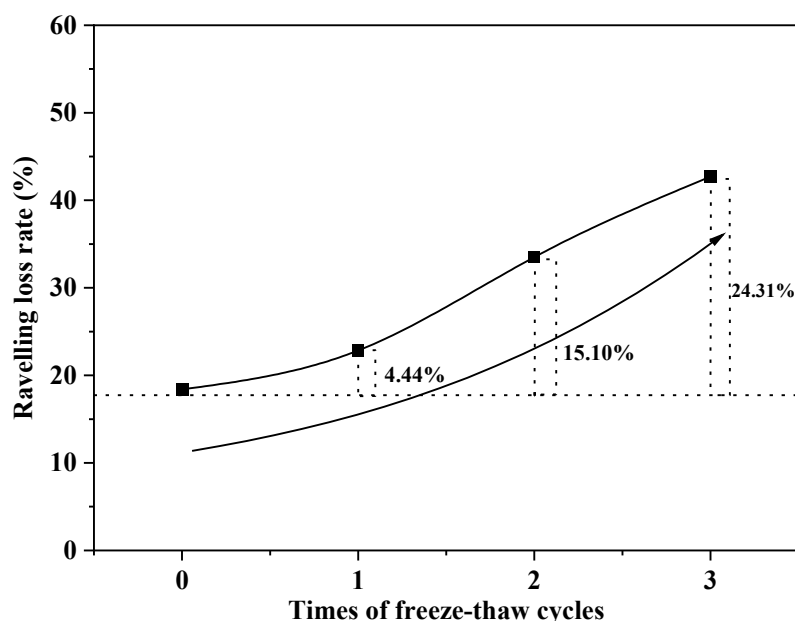


Figure 6. Effect of the freeze–thaw cycle test on the ravelling resistance performance of asphalt mixture.

3.1.3. Influence of Multiple Factors Based on UV Aging and Water Damage

Drainage asphalt pavements in service are affected by multiple factors. Therefore, to explore how the ravelling resistance performance of the drainage asphalt pavement attenuates in practical use, it is necessary to take light, heat, temperature, precipitation, and other factors into consideration in our test studies. The test results are an important basis for characterizing the ravelling performance of drainage asphalt pavements. The test results show (Figure 7) that with the same number of freeze–thaw cycles and the more the times of UV aging test cycles the greater the ravelling loss rate of asphalt Marshall specimens; with the same times of UV aging tests and the more the times of freeze–thaw cycles the greater the ravelling loss rate of asphalt Marshall specimens. The combined test of UV aging and freeze–thaw cycles aggravated the ravelling damage of asphalt specimens. The cohesiveness of the asphalt binders was damaged after the UV aging, and the interfacial adhesion between the binder and the aggregate was impaired. When immersion pressure and frost heave stress were further applied, the internal bonding properties of the asphalt specimens would dramatically decrease, thus, resulting in a greater Cantabro ravelling loss rate.

The results of the comparative analysis (Figures 5–7) show that in view of the damage of materials accelerated by environmental factors in nine UV aging tests combined, with one, two, and three times, respectively, of freeze–thaw cycle tests, for example, the Cantabro test, the ravelling loss rates of the specimens after the multiple factor accelerated damage process are 34.01%, 38.15%, and 54.24%, respectively. Compared with the standard specimens that have never undergone any aging tests, their ravelling loss rate increases by 15.61%, 19.75%, and 35.83%, respectively. However, with only the nine UV aging tests applied, the ravelling loss rate increases by 6.70% compared with the standard specimens. Furthermore, when only the one, two, and three times of freeze–thaw cycle tests are applied, respectively, the ravelling loss rate increased by 4.44%, 15.10%, and 24.31%, respectively, when compared with the standard specimens. It can be seen from the test results that the impact of the combined test of the UV aging and freeze–thaw cycles on the Cantabro ravelling loss rate of asphalt Marshall specimens is not a simple linear addition of the two aging test values. Most of the test data shows that the effect of the combined test on the asphalt specimens' ravelling loss rate exceeds the linear addition of the results of a single UV aging and single freeze–thaw cycle test, indicating that the combined test can exert aggravated damage on the asphalt specimens with a “ $1 + 1 > 2$ ” superimposed damage. This also shows that the drainage asphalt pavement in service under multiple complex

environments is more susceptible to the influence of various factors, which will lead to an accelerated attenuation of its ravelling performance.

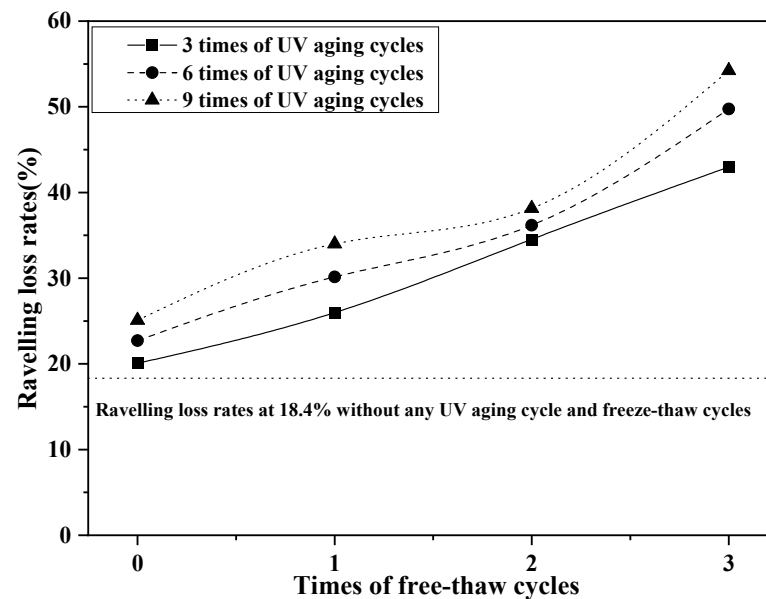


Figure 7. UV test results of the impact of the combined UV aging and freeze–thaw cycles.

To better explore the compound influence of the coupling effect of the UV aging and freeze–thaw cycle tests on the ravelling resistance performance of drainage asphalt pavement materials, the test data were fitted by using the Levenberg–Marquardt method, and the results are shown in Equation (1),

$$y = 16.54 + 1.16 \times x_1 + 4.86 \times x_2^{1.5}, \text{ correlation coefficient } R = 0.987 \quad (1)$$

where y is the Cantabro ravelling loss rate (%). x_1 is the times of UV aging tests (times). x_2 is the times of freeze–thaw cycle tests (times).

From the exponential function, it can be seen that the Cantabro ravelling loss rate of the asphalt mixture is well correlated with the times of UV aging and freeze–thaw cycles, and the times of freeze–thaw cycle tests have a greater influence on the asphalt mixture indicating that the attenuation law of the ravelling resistance performance of the drainage asphalt pavement material is consistent with the test findings. The exponential function in Equation (1) can be used to predict the ravelling loss rate of the asphalt mixture.

3.2. The Influence of Vehicle Factors on the Ravelling Resistance Performance of the Drainage Asphalt Pavement

3.2.1. Simulated Vehicle Speed Test—Rotating Surface Abrasion Speed Test

The test results of the simulated vehicle speed are shown in Figure 8. With the rotating speed increasing steadily, the ravelling loss rate of the trapezoidal plate tends to increase as a whole, and two inflection points appear in the test result graph. When the vehicle speed is at 40 r/min, the minimum ravelling loss rate of the trapezoidal plate specimen is 14.64% and the maximum ravelling loss rate of the trapezoidal plate is 33.60% at 100 r/min. The analysis concludes that high-speed rotation increases the shear stress and centrifugal force between the tire and the trapezoidal specimen, which intensifies the ravelling and stone loss on the surface of the trapezoidal plate, so the trapezoidal plate exhibits a larger ravelling loss rate under the high-speed rotation condition. The instantaneous contact pressure per unit area between the wheel and trapezoidal plate changes under the speed of 80 r/min. As a result, the asphalt specimen surface becomes weaker in resisting the wheel force and shows a decrease in its ravelling loss rate.

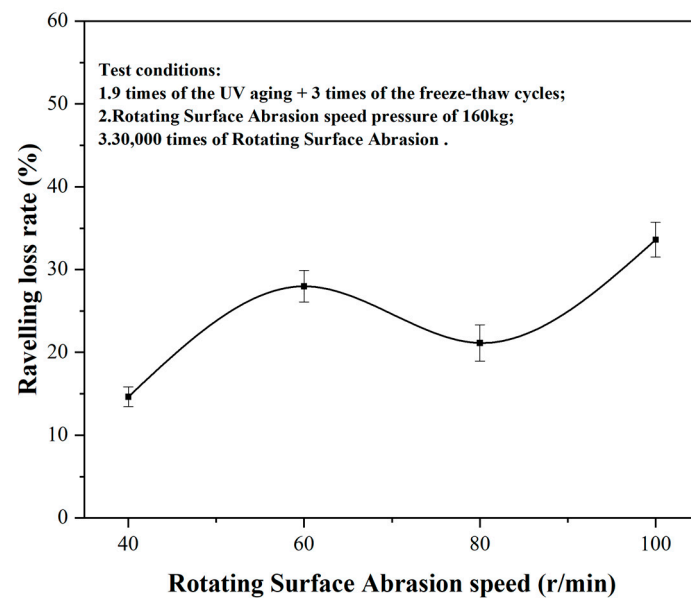


Figure 8. Simulated vehicle speed impact test.

3.2.2. Simulated Vehicle Load Test—Rotating Surface Abrasion Pressure Test

The test results show (Figure 9) that with the increase in the Rotating Surface Abrasion pressure the rotating ravelling loss rate of the trapezoidal specimens grows continuously, demonstrating an evident linear correlation. When the Rotating Surface Abrasion pressure increases to 160 kg, compared to 40 kg, the ravelling loss rate of trapezoidal plate specimens increases to more than 5 times, which shows that the Rotating Surface Abrasion pressure exacerbated the attenuation of asphalt specimens.

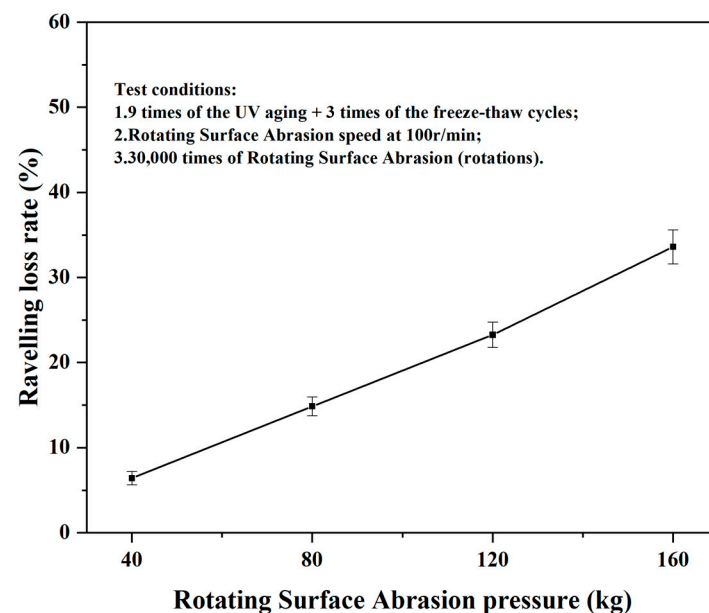


Figure 9. Simulated vehicle load impact test.

3.2.3. Simulated Traffic Volume Test—Rotating Surface Abrasion Test

The test results show (Figure 10) that with the increase in the Rotating Surface Abrasion times the rotating ravelling loss rate of asphalt trapezoidal specimens shows a growing tendency, demonstrating a more evident linear correlation. After comparing the result of the 30,000 times of Rotating Surface Abrasion with that of the 5000 times of Rotating Surface Abrasion, it can be found that the rotating ravelling loss rate of trapezoidal specimens

increases from 5.32% to 33.60%, showing an increase in more than 6 times. As seen from the test data, about every 5000 times of Rotating Surface Abrasion will cause the rotating ravelling loss rate of asphalt trapezoidal specimens to increase by 5%.

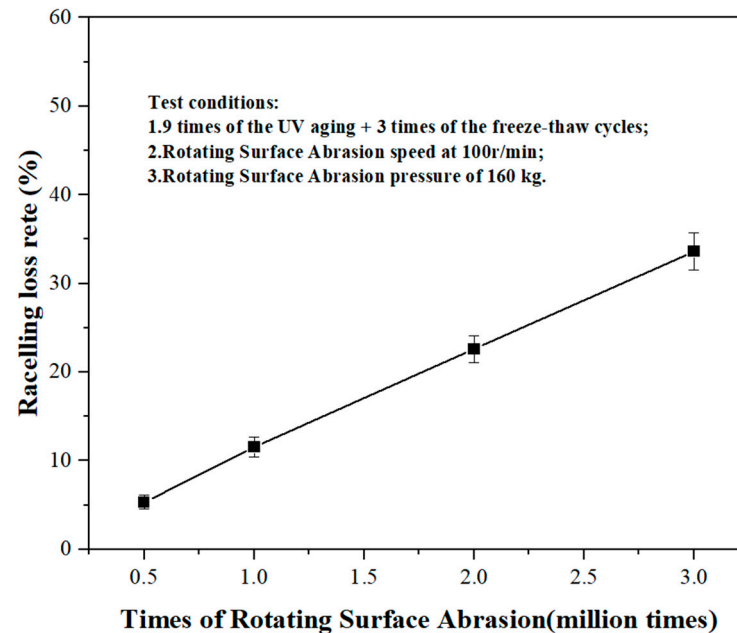


Figure 10. Test results of simulated traffic volume.

Above shows that the ravelling loss rate of the asphalt specimen is significantly affected by the times of Rotating Surface Abrasion, which also indicates that the traffic volume has a time-progressive impact on the ravelling resistance performance of the drainage asphalt pavement. With growing traffic volume and prolonged service time of the drainage asphalt pavement, the progressive effect of attenuation on the ravelling resistance performance of the drainage asphalt pavement is increasingly prominent. The drainage asphalt pavement is continuously worn and damaged by the heavy traffic on the road to the extent that the greater the traffic volume the greater the ravelling loss rate of the asphalt specimen materials.

3.3. Multi Factor Coupling Analysis

The analysis above has shown that vehicle speed, vehicle load, and traffic volume, among all the vehicle factors, have a more evident effect on the ravelling loss rate of the asphalt specimen, and the vehicle load and traffic volume also have a good linear relationship with the ravelling loss rate of the asphalt specimen. Therefore, to fit the data of the three vehicle factors with that of the rotating ravelling loss rate, Equation (2) can be established as follows.

$$y = 0.27 \times x_1 + 0.22 \times x_2 + 10.81 \times x_3 - 62.42, \text{ correlation coefficient } R = 0.964 \quad (2)$$

where:

y is the rotating ravelling loss rate (%).

x₁ is the Rotating Surface Abrasion speed (r/min).

x₂ is the Rotating Surface Abrasion pressure (kg).

x₃ is the times of Rotating Surface Abrasion (times).

It can be seen from Equation (2) that there exists a good correlation among the Rotating Surface Abrasion speed, pressure, times, and ravelling loss rate. In terms of the influence coefficient, the Rotating Surface Abrasion speed has a far greater impact on the rotating ravelling loss rate. This numerical analysis also shows that main vehicle factors such as vehicle

speed, vehicle load, and traffic volume accelerated the attenuation of the ravelling resistance performance of drainage asphalt pavements in actual operation, especially the traffic volume, which can produce more evident cumulative damage to the ravelling resistance performance as the service life of drainage asphalt pavements are continuously prolonged.

The results of the Rotating Surface Abrasion test and Cantabro Abrasion test are compared to collect some findings. Take the results of the most severe damage test for example, after nine times of the UV aging and three times of freeze–thaw cycles, under the condition that the Rotating Surface Abrasion speed is set at 100 r/min, pressure at 160 kg, and times at 30,000, the rotating ravelling loss rate of asphalt trapezoidal specimens is 33.60%, while under the same test conditions, under the condition that the Cantabro test speed is set at 30 r/min and 300 times, the Cantabro ravelling loss rate of the asphalt Marshall specimen is 54.24%. It can be seen that the results of the Cantabro Abrasion test are far bigger than that of the Rotating Surface Abrasion test due to the different principles of the two tests. In the Cantabro abrasion test, standard Marshall specimens were used in a cylindrical drum to carry out the test. The drum was rotating nonstop, and the Marshall specimens were forced to fall and crash against the cylindrical wall, which would greatly damage the surface and interior of the Marshall specimens. However, in the Rotating Surface Abrasion test, a simulated wheel–pavement contact test was adopted. During the test, the wheel only exerted a stripping damage effect on the surface of the trapezoidal plate specimen, to cause the difference between the two test results.

3.3.1. Single-Factor Influence

The regularity of the results obtained from the Cantabro and Rotating Surface Abrasion tests under the conditions of the single-factor influence was first explored, as shown in Figures 11 and 12. The test results show that with ever-increasing single-factor UV aging or freeze–thaw cycles, the ravelling loss rate obtained from both the Cantabro and rotating tests has the same growing tendency and have an evident correlation. Under the same single factor (UV aging or freeze–thaw cycles) influence, the loss rate obtained from the Cantabro Abrasion test is greater than that obtained from the Rotating Surface Abrasion test, which indicates that the Cantabro Abrasion test has a greater impact on the loss rate of asphalt specimens. This test not only produces ravelling of the surface of asphalt specimens, but also exerts a shock wave load on their internal structure resulting in aggravated damage. The effect of the Rotating Surface Abrasion test on the ravelling loss rate of asphalt specimens can better reflect the characteristics of the actual operating environment of the drainage asphalt pavement, showing that the vehicle tires have a greater impact on the ravelling resistance performance of the pavement's surface but milder damage to its internal structure.

The difference between the Cantabro ravelling loss rate and the rotating ravelling loss rate under the influence of the UV aging factor is relatively small (the maximum difference is 17.20%), while the difference between the ravelling loss rate obtained from the two tests under the influence of the freeze–thaw cycle factor is greater (the maximum difference is 29.11%). This indicates that the freeze–thaw cycle test has more serious damage to asphalt specimens on the one hand, and the Cantabro Abrasion test, on the other hand, accelerates the ravelling damage inside the asphalt specimens.

The analysis of test data obtained from the two stripping tests shows that the self-developed Rotating Surface Abrasion test has a good correlation with the Cantabro Abrasion test in conformity with the standard specification. Therefore, the test results of the Rotating Surface Abrasion test can be used to characterize the evolutionary law in the ravelling resistance performance of the drainage asphalt pavement surface. The self-developed Rotating Surface Abrasion test has two advantages. One is that it produces a smaller ravelling loss rate than the Cantabro Abrasion test under the same test conditions, and the other is that the self-developed Rotating Surface Abrasion test is more fitted to the changes of ravelling resistance performance of the drainage asphalt pavement's surface in service, while the Cantabro Abrasion test serves as a means to accelerate damage.

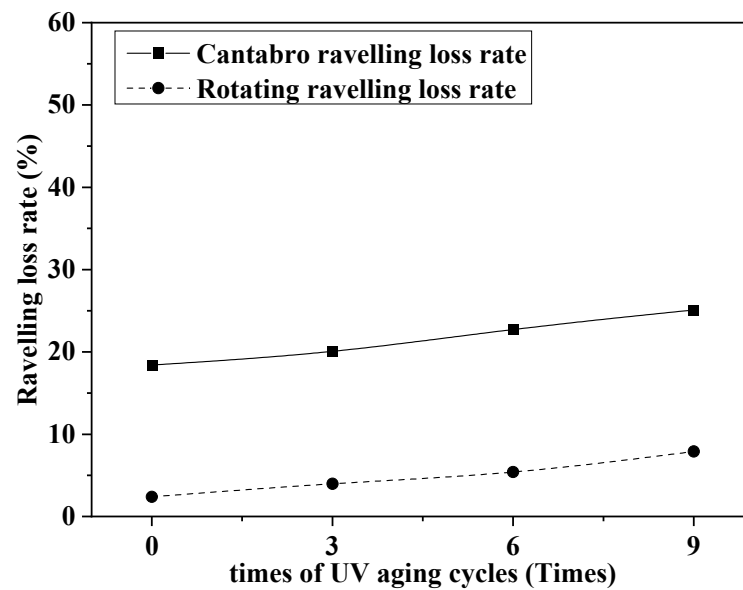


Figure 11. The results of the comparison between the two types of stripping tests under the influence of UV aging factors.

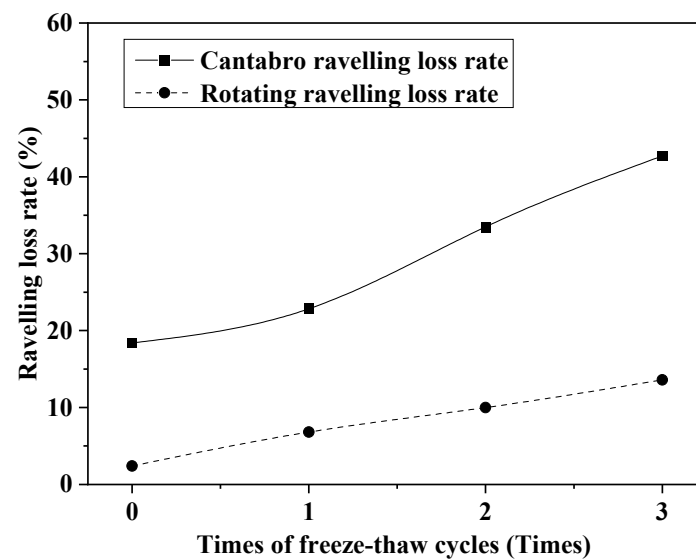


Figure 12. The results of the comparison between the two types of stripping tests under the influence of freeze–thaw cycle factors.

3.3.2. Multi-Factor Effects

To analyze the results obtained from the Cantabro abrasion and Rotating Surface Abrasion tests under the multiple-factor influence, the UV aging cycle test was first applied to asphalt specimens followed by the freeze–thaw cycle test. UV aging tests were taken three, six, and nine times, respectively, whereas freeze–thaw cycle tests were taken zero, one, two, and three times, respectively, so there were 12 groups of tests in total. The results of the comparison between the two stripping tests under the multiple-factor influence are shown in Figure 13.

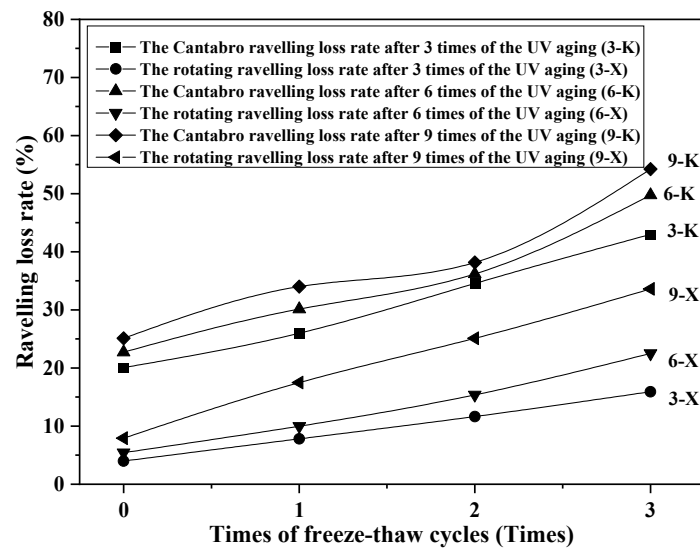


Figure 13. The results of the comparison between the two types of stripping tests under multi-factor influence.

The test results show that the ravelling loss rates obtained from the two tests are consistent in their changes under the multiple-factor influence of UV aging and freeze–thaw cycles, and the results of the two tests are well correlated. The greater the multiple-factor influence, the larger the ravelling loss rate of asphalt specimens obtained from both tests.

The above study confirms that the ravelling loss rates of asphalt specimens obtained from both Rotating Surface Abrasion and Cantabro Abrasion tests are well correlated. The test data from the two tests are fitted by adopting the Levenberg–Marquardt method combined with the general global optimization method to derive Equation (3), which is shown as follows.

$$y = 0.716 \times x - 10.702, \text{ correlation coefficient } R = 0.901 \quad (3)$$

where:

y is the rotating ravelling loss rate (%).

x is the Cantabro ravelling loss rate (%).

According to the test results shown in Figure 14, the two test results obtained from both the rotating and Cantabro Abrasion tests can be fitted to derive a linear function as the two results are well correlated. Therefore, this can provide a good theoretical and practical basis for selecting the Rotating Surface Abrasion test to evaluate the ravelling resistance performance of drainage asphalt pavements, thus, further proving the feasibility of applying the Rotating Surface Abrasion test index to characterize the attenuation law of the ravelling resistance performance of drainage asphalt pavements. Furthermore, as a simulated wheel–pavement contact is employed in the Rotating Surface Abrasion test, which can imitate the environment of drainage asphalt pavements in service, the effects of environmental factors such as light, heat, temperature, and water in UV aging and freeze–thaw cycles, as well as vehicle factors such as speed, vehicle load, and traffic volume, can better facilitate in the Rotating Surface Abrasion test, thus, confirming, both theoretically and practically, the applicability of the Rotating Surface Abrasion test index to the evolution of the ravelling resistance performance of the pavement’s surface.

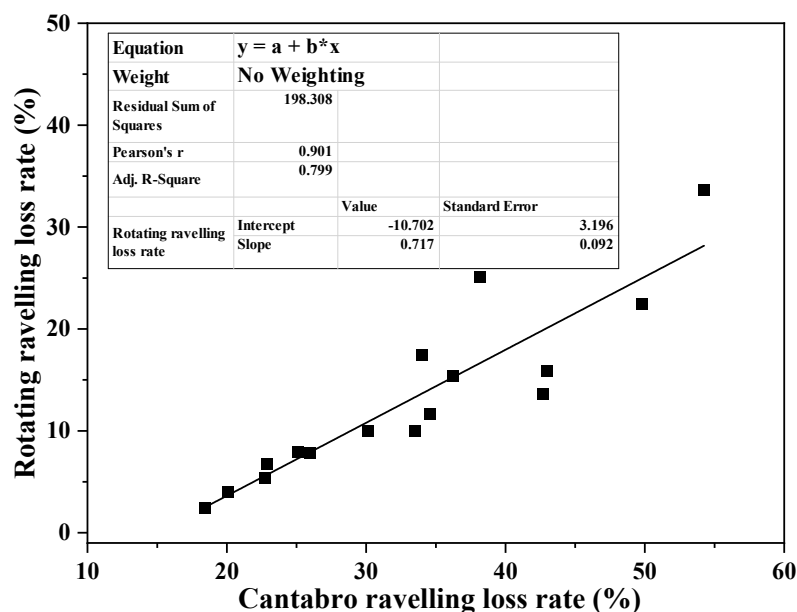


Figure 14. The correlation between the results of the Cantabro and Rotating Surface Abrasion tests.

4. Conclusions

In this study, numerous tests were conducted to find out the impact of environmental and vehicle factors on the ravelling resistance performance of drainage asphalt pavements. Meanwhile, the analysis of the correlation between the Cantabro Abrasion test and the Rotating Surface Abrasion tests was made. As a result, the influence of the law of complex service factors on the ravelling resistance performance of large-void asphalt pavements was clarified through the above test studies, and the main conclusions were drawn as follows.

- (1) With the increase in the times of UV aging cycles, the asphalt specimens show an increasing trend in the mass ravelling loss rate. The UV aging on asphalt pavements mainly impacts its surface area, ranging from the surface to about one centimeter below it.
- (2) With the same times of the UV aging and the increased times of freeze–thaw cycles the greater the ravelling loss rate of asphalt specimens.
- (3) The combined test of UV aging and freeze–thaw cycles aggravate the ravelling damage of asphalt specimens producing a “1 + 1 > 2” superimposed damage effect.
- (4) There exists a good correlation among the Rotating Surface Abrasion speed, pressure, times, and ravelling loss rate, and the Rotating Surface Abrasion times have a greater influence on the rotating ravelling loss rate.
- (5) The ravelling loss rates obtained from both the Cantabro and Rotating Surface Abrasion tests show a similar trend and have a good correlation.
- (6) The test results acquired from both the rotating and Cantabro Abrasion tests are fitted as linear functions with high correlation coefficients ($R = 0.901$), which confirms the feasibility of applying the Rotating Surface Abrasion test index to characterize the attenuation law of the ravelling resistance performance of drainage asphalt pavements.

Author Contributions: Conceptualization, Z.C.; methodology, Z.C.; software, S.Z.; validation, S.Z.; formal analysis, N.L.; investigation, X.L.; resources, X.L.; data curation, X.L.; writing—original draft preparation, L.L.; writing—review and editing, L.L.; visualization, N.L.; funding acquisition, Z.C. All authors have read and agreed to the published version of the manuscript.

Funding: The authors would like to acknowledge the support of the Science and Technology Innovation Project of Yunnan Communications Investment and Construction Group Co., Ltd. (YCIC-YF-2021-09), the Yunnan Key Laboratory of Digital Communications (grant No. 202205AG070008), the Science and Technology Innovation and Demonstration Project of Yunnan Provincial Department of Transportation (Yunjiaokejiaobian [2020]No.15-(1)), and the Independent Science and Technology Project of Yunnan Traffic Planning Design Research Institute Co., Ltd. (ZL-2021-02).

Institutional Review Board Statement: Not applicable.

Informed Consent Statement: Not applicable.

Data Availability Statement: Not applicable.

Conflicts of Interest: The authors declare no conflict of interest.

References

1. Chen, J.; Yin, X.; Wang, H.; Ding, Y. Evaluation of durability and functional performance of porous polyurethane mixture in porous pavement. *J. Clean. Prod.* **2018**, *188*, 12–19. [[CrossRef](#)]
2. Wang, X.; Gu, X.; Ni, F.; Deng, H.; Dong, Q. Rutting resistance of porous asphalt mixture under coupled conditions of high temperature and rainfall. *Constr. Build. Mater.* **2018**, *174*, 293–301. [[CrossRef](#)]
3. Gupta, A.; Rodriguez-Hernandez, J.; Castro-Fresno, D. Incorporation of additives and fibers in porous asphalt mixtures: A review. *Materials* **2019**, *12*, 3156. [[CrossRef](#)]
4. Arshad, A.; Ahmad, J.; Masri, K. Rutting resistance of nanosilica modified porous asphalt. *Int. J. Civ. Eng. Technol.* **2019**, *10*, 2274–2284.
5. Hu, M.; Li, L.; Peng, F. Laboratory investigation of OGFC-5 porous asphalt ultra-thin wearing course. *Constr. Build. Mater.* **2019**, *219*, 101–110. [[CrossRef](#)]
6. Shirini, B.; Imaninasab, R. Performance evaluation of rubberized and SBS modified porous asphalt mixtures. *Constr. Build. Mater.* **2016**, *107*, 165–171. [[CrossRef](#)]
7. Lyons, K.R.; Putman, B.J. Laboratory evaluation of stabilizing methods for porous asphalt mixtures. *Constr. Build. Mater.* **2013**, *49*, 772–780. [[CrossRef](#)]
8. Rodriguez-Hernandez, J.; Andrés-Valeri, V.C.; Calzada-Pérez, M.A.; Vega-Zamanillo, Á.; Castro-Fresno, D. Study of the raveling resistance of porous asphalt pavements used in sustainable drainage systems affected by hydrocarbon spills. *Sustainability* **2015**, *7*, 16226–16236. [[CrossRef](#)]
9. Shen, D.-H.; Wu, C.-M.; Du, J.-C. Laboratory investigation of basic oxygen furnace slag for substitution of aggregate in porous asphalt mixture. *Constr. Build. Mater.* **2009**, *23*, 453–461. [[CrossRef](#)]
10. Wang, T.; Dra, Y.A.S.S.; Cai, X.; Cheng, Z.; Zhang, D.; Lin, Y.; Yu, H. Advanced cold patching materials (CPMs) for asphalt pavement pothole rehabilitation: State of the art. *J. Clean. Prod.* **2022**, *366*, 133001. [[CrossRef](#)]
11. Luo, S.; Lu, Q.; Qian, Z. Performance evaluation of epoxy modified open-graded porous asphalt concrete. *Constr. Build. Mater.* **2015**, *76*, 97–102. [[CrossRef](#)]
12. Wang, T.; Weng, Y.; Cai, X.; Li, J.; Xiao, F.; Sun, G.; Zhang, F. Statistical modeling of low-temperature properties and FTIR spectra of crumb rubber modified asphalts considering SARA fractions. *J. Clean. Prod.* **2022**, *374*, 134016. [[CrossRef](#)]
13. Xu, B.; Li, M.; Liu, S.; Fang, J.; Ding, R.; Cao, D. Performance analysis of different type preventive maintenance materials for porous asphalt based on high viscosity modified asphalt. *Constr. Build. Mater.* **2018**, *191*, 320–329. [[CrossRef](#)]
14. Miradi, M. In Extraction of rules from artificial neural network for dutch porous asphalt concrete pavement. In Proceedings of the 2007 International Joint Conference on Neural Networks, Orlando, FL, USA, 12–17 September 2007; IEEE: New York, NY, USA, 2007; pp. 1853–1858.
15. Zhang, Y.; Li, H.; Lu, Q.; Yang, J.; Wang, T. Effect of Different Admixtures on Pore Characteristics, Permeability, Strength, and Anti-Stripping Property of Porous Concrete. *Buildings* **2022**, *12*, 1020. [[CrossRef](#)]
16. Zhang, H.; Li, H.; Zhang, Y.; Wang, D.; Harvey, J.; Wang, H. Performance enhancement of porous asphalt pavement using red mud as alternative filler. *Constr. Build. Mater.* **2018**, *160*, 707–713. [[CrossRef](#)]
17. Hu, J.; Ma, T.; Zhu, Y.; Huang, X.; Xu, J.; Chen, L. High-viscosity modified asphalt mixtures for double-layer porous asphalt pavement: Design optimization and evaluation metrics. *Constr. Build. Mater.* **2021**, *271*, 121893. [[CrossRef](#)]
18. Mabui, D.; Tjaronge, M.; Adisasmitha, S.; Pasra, M. Performance of porous asphalt containing modified Buton asphalt and plastic waste. *GEOMATE J.* **2020**, *18*, 118–123. [[CrossRef](#)]
19. Herrington, P.; Reilly, S.; Cook, S. *Porous Asphalt Durability Test*; Transfund: Lower Hutt, New Zealand, 2005.
20. Mousavi Rad, S.; Kamboozia, N.; Anupam, K.; Saed, S.A. Experimental Evaluation of the Fatigue Performance and Self-Healing Behavior of Nanomodified Porous Asphalt Mixtures Containing RAP Materials under the Aging Condition and Freeze–Thaw Cycle. *J. Mater. Civ. Eng.* **2022**, *34*, 04022323. [[CrossRef](#)]
21. Dan, H.-C.; Ling, C.; Cao, W.; Wang, Z.; Liu, J. Fatigue behavior and phenomenological modeling of porous asphalt concrete under freeze–thaw cycling. *Mater. Struct.* **2021**, *54*, 1–11. [[CrossRef](#)]

22. Vallerga, B.; Monismith, C.; Granthem, K. In A study of some factors influencing the weathering of paving asphalts. *Assoc. Asphalt Paving Technol. Proc.* **1957**, *26*, 126.
23. Tu, J.; Yuan, J.; Bao, C.; Cheng, J. Study on ultraviolet radiation aging of road asphalt and SBS modified asphalt. *Pet. Asph.* **2008**, *22*, 43–47.
24. Diao, L.; Gu, S.; Wang, P. Measurements and analyses on Beijing ground surface ultraviolet radiation (spectrum). *Sci. Meteorol. Sin.* **2003**, *23*, 22–30.
25. Fan, T.-J.; Tian, W.-Y.; Xu, D.-L. Influence of mix proportion on abrasion and stripping characteristics of drainage asphalt pavement. *Jianzhu Cailiao Xuebao (J. Build. Mater.)* **2007**, *10*, 435–439.
26. Moore, L.M.; Hicks, R.; Rogge, D.F. Design, construction, and maintenance guidelines for porous asphalt pavements. *Transp. Res. Rec.* **2001**, *1778*, 91–99. [[CrossRef](#)]
27. Caro, S.; Masad, E.; Bhasin, A.; Little, D.N. Moisture susceptibility of asphalt mixtures, Part 1: Mechanisms. *Int. J. Pavement Eng.* **2008**, *9*, 81–98. [[CrossRef](#)]
28. Mehrara, A.; Khodaii, A. A review of state of the art on stripping phenomenon in asphalt concrete. *Constr. Build. Mater.* **2013**, *38*, 423–442. [[CrossRef](#)]
29. Ma, X.; Li, Q.; Cui, Y.-C.; Ni, A.-Q. Performance of porous asphalt mixture with various additives. *Int. J. Pavement Eng.* **2018**, *19*, 355–361. [[CrossRef](#)]
30. Mabui, D.; Tjaronge, M.; Adisasmitha, S.; Pasra, M. Resistance to cohesion loss in cantabro test on specimens of porous asphalt containing modified asbuton. In Proceedings of the IOP Conference Series: Earth and Environmental Science, Changchun, China, 21–23 August 2020; IOP Publishing: Bristol, UK, 2020; p. 012100.
31. Badeli, S.; Carter, A.; Dore, G. Effect of laboratory compaction on the viscoelastic characteristics of an asphalt mix before and after rapid freeze-thaw cycles. *Cold Reg. Sci. Technol.* **2018**, *146*, 98–109. [[CrossRef](#)]

Disclaimer/Publisher’s Note: The statements, opinions and data contained in all publications are solely those of the individual author(s) and contributor(s) and not of MDPI and/or the editor(s). MDPI and/or the editor(s) disclaim responsibility for any injury to people or property resulting from any ideas, methods, instructions or products referred to in the content.